

# Considering Aerosol Processes in Nuclear Transport Package Containment Safety Cases

Andrew Cummings, Rhianne Boag, Sarah Bryson, Gordon Turner

**Abstract**—Packages designed for transport of radioactive material must satisfy rigorous safety regulations specified by the International Atomic Energy Agency (IAEA). Higher Activity Waste (HAW) transport packages have to maintain containment of their contents during normal and accident conditions of transport (NCT and ACT). To ensure containment criteria is satisfied these packages are required to be leak-tight in all transport conditions to meet allowable activity release rates. Package design safety reports are the safety cases that provide the claims, evidence and arguments to demonstrate that packages meet the regulations and once approved by the competent authority (in the UK this is the Office for Nuclear Regulation) a licence to transport radioactive material is issued for the package(s). The standard approach to demonstrating containment in the RWM transport safety case is set out in BS EN ISO 12807. In this document a method for measuring a leak rate from the package is explained by way of a small interspace test volume situated between two O-ring seals on the underside of the package lid. The interspace volume is pressurised and a pressure drop measured. A small interspace test volume makes the method more sensitive enabling the measurement of smaller leak rates. By ascertaining the activity of the contents, identifying a releasable fraction of material and by treating that fraction of material as a gas, allowable leak rates for NCT and ACT are calculated. The adherence to basic safety principles in ISO12807 is very pessimistic and current practice in the demonstration of transport safety, which is accepted by the UK regulator. It is UK government policy that management of HAW will be through geological disposal. It is proposed that the intermediate level waste be transported to the geological disposal facility (GDF) in large cuboid packages. This poses a challenge for containment demonstration because such packages will have long seals and therefore large interspace test volumes. There is also uncertainty on the releasable fraction of material within the package ullage space. This is because the waste may be in many different forms which makes it difficult to define the fraction of material released by the waste package. Additionally because of the large interspace test volume, measuring the calculated leak rates may not be achievable. For this reason a justification for a lower releasable fraction of material is sought. This paper considers the use of aerosol processes to reduce the releasable fraction for both NCT and ACT. It reviews the basic coagulation and removal processes and applies the dynamic aerosol balance equation. The proposed solution includes only the most well understood physical processes namely; Brownian coagulation and gravitational settling. Other processes have been eliminated either on the basis that they would serve to reduce the release to the environment further (pessimistically in keeping with the essence of nuclear transport safety cases) or that they are not credible in the conditions of transport considered.

**Keywords**—Aerosol processes, Brownian coagulation, gravitational settling, transport regulations.

Andrew Cummings and Rhianne Boag are with International Nuclear Services, Hinton House, Birchwood Park Avenue, Warrington, WA3 6GR, e-mail: andrew.cummings@innuserv.com

Gordon Turner and Sarah Bryson are with Radioactive Waste Management, Building 587, Curie Avenue, Harwell Campus, Didcot, OX11 0RH

## I. INTRODUCTION

THE Nuclear Decommissioning Authority (NDA) are responsible for decommissioning of the UK's civil nuclear legacy. Two of their subsidiaries have key roles in supporting this objective; Radioactive Waste Management (RWM) and International Nuclear Services (INS). RWM are tasked with delivering a geological disposal facility whilst INS provide nuclear transport solutions. INS are contracted by RWM to integrate nuclear transport with possible geological disposal options. To this end RWM have tasked INS with developing transport packages for HAW that satisfy nuclear transport regulations and can be operated at a GDF. Fig. 1 shows a computer model of a concept transport package design. The main transport package that is being developed to fulfil this role is the Standard Waste Transport Container (SWTC). The SWTC is of cuboid shape and sized to fit in the most restrictive rail gauge within the UK. The transport package dimensions are approximately 2.4 m (*width*) x 2.4m (*breadth*) x 2.2 m (*height*).

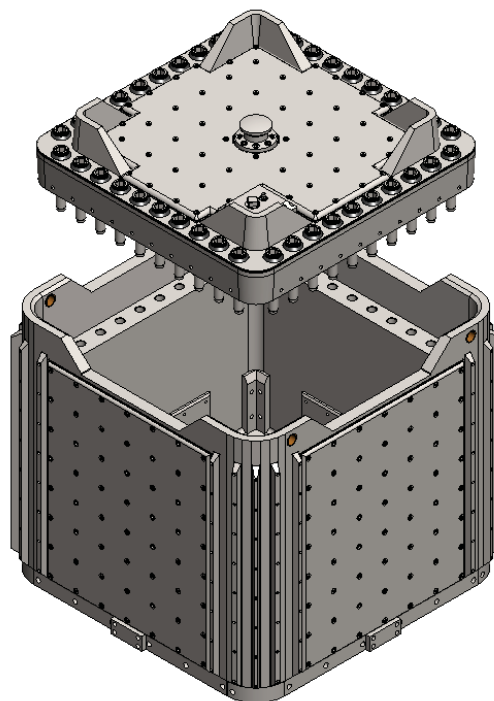


Fig. 1 Concept transport package design

The SWTC will be loaded with various waste packages

filled with HAW. The waste packages vary in form; some are stainless steel clad boxes and others are drums. The HAW inside of the waste package is conventionally immobilised with cement and a capping grout and innovative solutions are being considered to assess the viability of packaging HAW in alternative ways. Fig. 2 shows a sectioned transport package loaded with 4 x 500 litre stainless steel clad drums. To satisfy the IAEA Regulations for the Safe Transport of Radioactive Material [1] transport packages (e.g. SWTC) must maintain containment in all conditions. The containment success criteria is provided as an activity release rate and there are two different rates for normal and accident conditions of transport (NCT and ACT). The waste material consists of a mixture of radionuclides and the Transport Regulations [1] introduce the  $A_2$  value to quantify the amount of activity within individual waste packages. During NCT the permissible activity release rate for Type B packages (such as the SWTC) is  $1 \times 10^{-6} A_2/\text{hr}$ , whereas during ACT the permissible activity release rate is  $1 \times A_2/\text{week}$  [1, 2] (except for  $^{85}\text{Kr}$  which is  $10 \times A_2/\text{week}$ ).

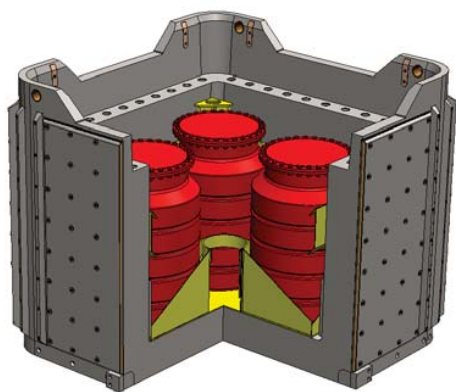


Fig. 2 Sectioned transport package loaded with 4 x 500 litre waste packages (drums)

The standard approach to demonstrating containment of transport packages to the regulator is described in BS EN ISO12807 [2]. The first step is to determine the activity content of the waste to be transported in terms of  $A_2$ 's and then identify a releasable fraction of material which is assumed to be in gas suspension within the ullage space and potential for release to the environment. By treating this fraction of solid particulate as a fraction of the ullage space gas a permissible activity release rate is calculated and subsequent calculations provide a permissible standardised leakage rate (SLR). To complete the demonstration a leakage test is then performed to compare the measured leakage rate to the permissible rate. This is carried out on larger packages using a pressure drop (or rise) test. Here the focus is directed on the pressure drop test but the discussion is also relevant to a pressure rise test.

A pressure drop test involves pressurising a small interspace test volume which is designed between the package lid and body with double, dove-tail grooves on the underside of the lid and elastomeric, O-ring seals fitted within the grooves, Fig. 3). The pressure drop is then measured and a leakage rate determined.

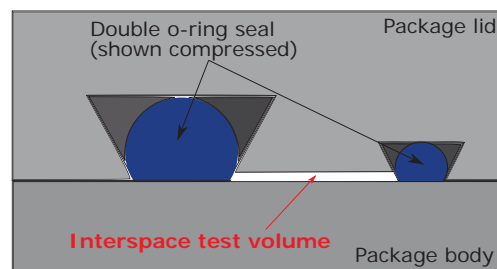


Fig. 3 Interspace test volume situated between double O-ring seal configuration. The larger seal is the containment seal i.e. the barrier between the radioactive particles and the environment, and the second seal provided for test purposes to verify the containment

A drawback of both methods is that to measure small leakage rates the interspace test volume needs to be small itself. This is because a larger test volume is sensitive to temperature changes, therefore limiting the volume enables smaller leakage rates to be detected. In the case of the SWTC the interspace test volume is larger than desirable due to the size of the waste packages to be transported which result in a transport package with a long seal and therefore a large interspace test volume. As a consequence measuring small leakage rates to demonstrate containment poses a potential problem for the safety case.

Work is currently underway to characterise the activity of the waste inventory and understand how much of the waste may not be suitable for simply treating as a gas. This screening of the waste includes assessing the known and unknown radionuclides present, their mass fractions and their phase for groups of waste packages. The present work focuses on understanding the releasable fraction and its airborne lifetime during NCT and ACT.

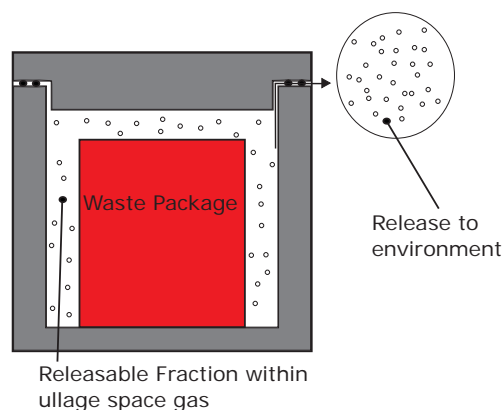


Fig. 4 Releasable fraction of particulate within ullage space and potential release route to the environment

Fig. 4 shows a schematic of the releasable fraction within the transport package ullage space and its potential release route to the environment. It is proposed that the releasable fraction during NCT is derived from surface contamination limits. The regulations provide a maximum permissible surface contamination limit in Becquerels per square centimetre ( $\text{Bq}/\text{cm}^2$ ). Tests are carried out prior to loading within a transport package to determine if surface contamination is

acceptable. Therefore it is conservative to assume that the maximum possible surface contamination is available for release within the ullage space gas.

Transport package acceptance criteria for ACT is based on satisfactory performance accounting for cumulative damage from the following tests:-

- 0.3 m accidental handling drop (applicable to these packages due to their mass)
- 9 m drop onto an unyielding target in the most onerous orientation
- 1 m drop onto a mild steel punch in the most onerous position and orientation
- 800 °C all engulfing pool fire for 30 minutes and subsequent cooling<sup>1</sup>

It is proposed that the releasable fraction for ACT is taken from results of a drop testing programme for a variety of waste packages dropped from various heights greater than 9 m. As the drop height was increased in most cases above 9 m during the tests, the results may be considered a bounding case. In fact many of the waste packages did not rupture during those tests but they are not designed to be a demonstrable containment boundary that satisfies transport regulations. Therefore, in keeping with nuclear safety principles they are not relied upon in the containment argument. It is currently assumed that no further release fraction occurs during the thermal accident.

In the NCT case the proposed use of surface contamination limits bounds the uncertainty in a conservative way. For ACT the large number of waste packages, their differing integrity and their content and composition makes the releasable fraction more difficult to precisely define.

Guidance notes provided in ISO12807 state that the releasable fraction depends on the mobility of aerosols or particulates [2]. The following approach focuses on how aerosol dynamics can be used to safely reduce the releasable fraction.

## II. BACKGROUND

Friedlander [3] and Williams [4, 5] provide good starting points for applying aerosol science methods to assess nuclear containments. Central to these methods is the dynamic aerosol balance equation that enables consideration of all potential aerosol processes acting in any environment - once some simplifications have been made [4]. This has been successfully applied in the PHEBUS project by several authors [6–8]. In particular the work carried out by Cousin et al. [6] provides a summary of the aerosol phenomena acting during a severe accident in a water cooled nuclear reactor. A state of the art overview of aerosol phenomena acting during reactor containments is provided by Allelein et al. [9].

Work on nuclear packages or storage casks has focused on the aerosol behaviour in and around the leakage path. For example Chatzidakis [10] considered spent fuel casks used for long term dry storage of radioactive material. If subjected to

stress corrosion cracking the spent fuel casks have a potential leak pathway. Chatzidakis [10] applied the dynamic aerosol balance equation to model the processes occurring within the leak pathway and to calculate its reduction in cross sectional area. He concluded that further work should be carried out to understand whether deposition in the leak paths can also result in plugging of the leak path but modelling showed little release of aerosol for leak paths (cracks)  $< 50 \mu\text{m}$ .

Clement [11] carried out theoretical work on capillary blockage (or plugging) in laminar gas flow. He concluded that fine capillaries will not always become plugged and in certain gas flow conditions aerosol penetration will be very efficient. However, small changes to the gas flow can lead to rapid capillary plugging. Morton et al. [12] carried out experimental work on the influence of pressure on aerosol penetration through capillary leaks and drew similar conclusions to Clement [11]. Their data indicated that at large pressure differentials ( $\geq 80 \text{kPa}$ ) virtually no plugging occurred and the aerosol penetrated the capillary efficiently. Conversely as the pressure differential reduced attenuation of aerosol release occurred. Tian et al. [13] carried out a similar experimental study on thin capillaries and fine particles. Their conclusions were in-keeping with Clement [11] and Morton [12]; that smaller particles have a good ability to penetrate capillaries, pressure differential is very important to penetration efficiency and shorter capillaries are less prone to plugging than longer ones. They also found that at constant pressure and capillary length the leakage of particles was invariant to capillary diameter.

Martens et al. [14] have carried out a programme of work on characterising the releasable fraction (source term) of low specific activity brittle/powdery materials. Their study involved the development of a novel method to measure particle size distributions post accident to satisfy the IAEA Regulations [1] for lower activity packages known as type A's. Koch et al. [15] devised an experiment suitable for determining the releasable fraction of a wide class of brittle radioactive materials. Martens [14] determined the release fractions and size distributions for pulverised fly ash and Titanium dioxide ( $\text{TiO}_2$ ) surrogate materials.

## III. MODELLING AEROSOL BEHAVIOUR INSIDE A NUCLEAR TRANSPORT PACKAGE

The dynamic aerosol balance equation is written as [4]:-

$$\frac{\partial n(v, t)}{\partial t} + R(v, t)n(v, t) + \frac{\partial}{\partial v}(I(v, t)n(v, t)) = \frac{1}{2} \int_0^v du K(u, v-u)n(u, t)n(v-u, t) - n(v, t) \int_0^\infty du K(u, v)n(u, t) + S(v, t) \quad (1)$$

where the 1st term on the left hand side represents the change in particle number with respect to time, the second term represents removal mechanisms i.e. gravitational settling, leakage and deposition. The third term describes the effects of condensation and evaporation, the fourth and fifth terms

<sup>1</sup> It is noteworthy that the concept SWTC design is 285 mm wall thickness and therefore the effects of the fire on the waste package occur after the 30 minute fire and increase the peak internal temperature and pressure to 160 °C and 20 barg respectively.

combined represent coagulation i.e. Brownian, turbulent, gravitational and the final term is the source term.

Whilst implementing the model for transport package containment only the terms (and therefore physical processes) required to meet activity release rates are included and all other terms are excluded. The selection of which terms to include in the model is discussed in the following sections.

#### A. Coagulation

Coagulation is the process of particles colliding and sticking together resulting on particle growth. Attractive van der Waals forces are ever present and serve to enhance coagulation. There is also potential for repulsive electrostatic forces to act on particles which may reduce the efficiency of collisions resulting in attenuation of the coagulation rate. Additionally inertial forces can act both for and against coagulation depending on the flow circumstances (e.g. turbulence) and therefore presents potential to decrease coagulation rate.

1) *Brownian Coagulation:* Brownian motion is ever present and occurs over small length scales and times irrespective of gas flow. At very small length scales the Knudsen number increases above 1 and the distance between the carrier gas molecules and the entrained particles becomes large. In these circumstances the flow regime is referred to as free molecular. Brownian coagulation can be modelled in the free molecular regime with [4]:-

$$K_{FM}(a, b) = \left(\frac{6kT}{\rho}\right)^{1/2} (a + b)^2 \left(\frac{1}{a^3} + \frac{1}{b^3}\right)^{1/2} \quad (2)$$

where

$a, b$  = Particle radius  $a$  and  $b$

$k$  = Boltzmanns constant  $1.38 \times 10^{-23}$  J/K

$T$  = Carrier gas temperature

$\rho$  = Particle density

When the Knudsen number falls below 1 and the particles more readily collide with the carrier gas the flow is referred to as the continuum regime. Brownian coagulation in the continuum regime is modelled with the following coagulation kernel [4]:

$$K_B(a, b) = \frac{2kT}{3\mu} \left(\frac{1}{a} + \frac{1}{b}\right) (a + b) \quad (3)$$

where  $\mu$  is the dynamic viscosity of the carrier gas.

In the case when a transition between continuum and free molecular regime occurs the Cunningham correction can be applied by modifying the diffusion coefficient as [4]:-

$$D_a = D_B C_a \quad \text{where } D_B = \frac{kT}{6\pi a \mu} \quad (4)$$

and [4]:-

$$C_a = 1 + Kn \left[ A + B \exp\left(-\frac{E}{Kn}\right) \right] \quad (5)$$

where  $A=1.257$ ,  $B=0.4$  and  $E = 1.1$  [4]. The Knudsen number (Kn) is the ratio of the mean free path of the carrier gas

molecules (in this case air) to the particle size (radius). This correction leads to a modified Brownian coagulation kernel [4]:-

$$K_B(a, b) = \frac{2kT}{3\mu} \left(\frac{C_a}{a} + \frac{C_b}{b}\right) (a + b) \quad (6)$$

Since the mean free path of air is pressure and temperature dependant it has been evaluated by calculating the molecular density of air [3]:-

$$\rho_m = \frac{p}{kT} \quad (7)$$

and then finding the mean free path,  $l_p$  as [3]:-

$$l_p = \frac{0.707}{\pi \rho_m \sigma_{air}^2} \quad (8)$$

where  $\sigma_{air}$ , the molecular diameter of air molecules, is taken as  $0.37 \times 10^{-9}$   $\mu\text{m}$  [16].

The Knudsen number is then found from [3]:-

$$Kn = \frac{l_p}{a} \quad (9)$$

These coagulation kernels have been numerically evaluated using a test particle with a diameter of  $1.0 \mu\text{m}$ . Fig. 5 shows the results generated at standard temperature and pressure (STP) and at the peak temperature and pressure expected during ACT. It is evident that the lowest coagulation rate is due to Brownian coagulation in the continuum regime, therefore this kernel only is selected for incorporation into the model as it is the most conservative with respect to a potential activity release to the environment.

2) *Turbulent Coagulation:* Two mechanisms are responsible for turbulent coagulation; diffusion (or shear) and inertial turbulence. They often occur simultaneously and their effects are different depending on particle size. Turbulent diffusion is described by Williams [4] as a macroscopic Brownian motion where smaller particles become entrained in turbulent eddies resulting in collisions. Turbulent inertial coagulation tends to affect larger particles that, due to their inertia are not fully entrained in the turbulent eddies. These local increases in acceleration of the gas are transmitted to the particles resulting in increased collisions.

The turbulent diffusion coagulation kernel is [4]:-

$$K_{TD}(a, b) = 5.65 \left(\frac{\epsilon_T}{\nu}\right)^{1/2} (a + b)^3 \quad (10)$$

where:-

$\epsilon_T$  = turbulent intensity

$\nu$  = Kinematic viscosity

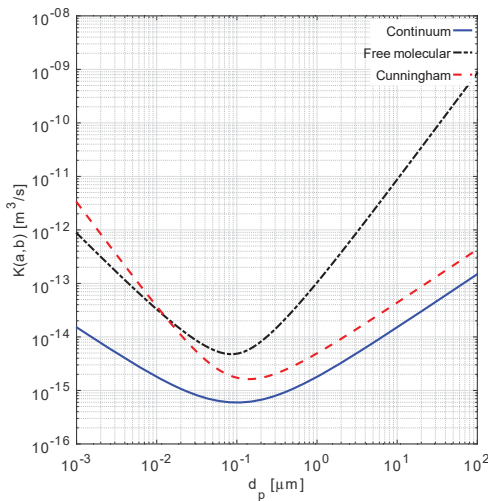
and [4]:-

$$\epsilon_T = \frac{\bar{u}}{l^3} \quad (11)$$

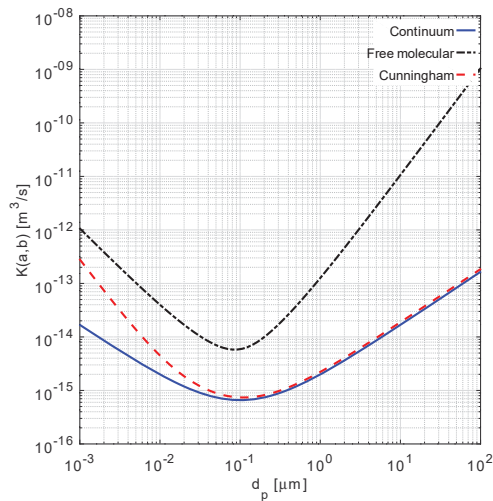
where the root mean square velocity,  $\bar{u}$ , is taken as  $0.5 \text{ m/s}$  and the length scale of turbulent eddies is taken as 10% of the containment length  $0.07 \text{ m}$  for the present assessment.

The turbulent inertial coagulation kernel is [4]:-





(a) Numerically evaluated at STP



(b) Numerically evaluated at ACT temperature and pressure

Fig. 5 Brownian coagulation - comparison of kernels in the continuum and free molecular regime and corrected with the Cunningham factor for Knudsen numbers between 1 and 10

$$K_{TI} = 6.2 \frac{\epsilon^{3/4}}{\nu^{1/4}} (a+b)^2 |\tau_a - \tau_b| \text{ where } \tau_a = \frac{2\rho_p a^2}{9\mu} \quad (12)$$

As the length and timescales associated with turbulent coagulation are much greater than that of Brownian coagulation the two mechanisms coexist. Smaller particles are less influenced by turbulent coagulation as they do not become entrained in the turbulence due to the disparity between the microscale of turbulence ( $100\mu\text{m} - 500\mu\text{m}$  [4]) and particle size. Therefore there is a critical size of particle when turbulent coagulation becomes significant. Williams states that the critical particle size at STP is  $1\mu\text{m}$  [4]. This is supported by Friedlander [3] and appears to be a lower bound when compared to the work of Park et al. [17] who calculated the critical size of particles is between  $2 - 20\mu\text{m}$ .

3) *Gravitational Coagulation*: The final coagulation mechanism is gravity that acts simultaneously with Brownian and turbulent coagulation.

The gravitational coagulation kernel is [4]:-

$$K_g(a, b) = \pi g(a+b)^2 |\tau_a - \tau_b| \quad (13)$$

To compare the rates of coagulation due to gravity, turbulence and Brownian motion the kernels have been evaluated numerically and are plotted in Fig. 6. It is noteworthy that in reality Brownian motion and gravity are ever present and will act simultaneously, and if turbulent flow is present this will also act in combination with these mechanisms. The net effect of this is that the rate of coagulation is increased by accounting for all mechanisms but in the proposed approach only Brownian coagulation in the continuum regime is modelled. This will result in conservative calculations for the release to the environment.

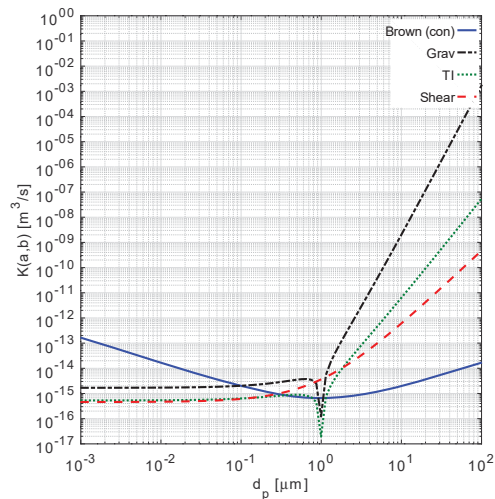


Fig. 6 Comparison of the rates of coagulation due to Brownian (continuum), turbulent (inertial and diffusion) and gravitational coagulation (Test particle  $1\mu\text{m}$ )

The fact that the three coagulation processes can occur simultaneously makes the choice of only the weakest mechanism (Brownian coagulation in the continuum regime) highly conservative. It is evident that above the critical particle size turbulent coagulation (and gravitational) would greatly increase the rate of coagulation and reduce the release of activity to the environment.

4) *Collision Efficiency*: All of the kernels discussed assume that particles instantaneously stick upon collision. Interparticle forces determine whether instantaneous sticking occurs; these generally arise from electrical effects, inertial effects and surface forces. When particles carry electrical charge or are subjected to external viscous forces their collision efficiency

may decrease. On the other hand London-van der Waals surface forces attract particles and serve to enhance collision efficiency [3]. An extensive study has been carried out by Shahub and Williams [18, 19] on the effects of collision efficiency on Brownian coagulation in the continuum regime. They concluded that a collision efficiency of 0.51 constitutes a lower bound therefore this value has been adopted in the present model. This is introduced in 3 as a multiplication factor.

5) *Spherical Particles*: An implicit assumption in all the kernels presented is that the particles are perfectly spherical. Although this is true for liquids this is unlikely to be the case for solid particulate that often tend towards chain like structures. Friedlander classifies solid growth of particles in the size range of 100nm to a few microns as agglomeration [3]. It has been found experimentally that the total number of primary particles in an agglomerate obeys a power law relationship:-

$$n \approx R^{D_f} \quad (14)$$

where:-

$$\begin{aligned} n &= \text{Number of particles} \\ R &= \text{Characteristic radius} \\ D_f &= \text{Fractal dimension} \end{aligned}$$

For spherical particles (or compact particles)  $D_f \rightarrow 3$  whilst for chain-like structures  $D_f \rightarrow 1$  [3].

The modified Brownian coagulation kernel (continuum) is written in terms of particle volume as [3]:-

$$K(v_i, v_j) = \frac{2k_B T}{3\mu} \left( \frac{1}{v_i^{1/D_f}} + \frac{1}{v_j^{1/D_f}} \right) (v_i^{1/D_f} + v_j^{1/D_f}) \quad (15)$$

When  $D_f=3$  the equation reduces back to the Brownian coagulation kernel in the continuum regime. Fig. 7 indicates that the rate of coagulation for non-spherical particles is always greater than for spherical particles therefore the selection of the unmodified continuum Brownian coagulation kernel is conservative.

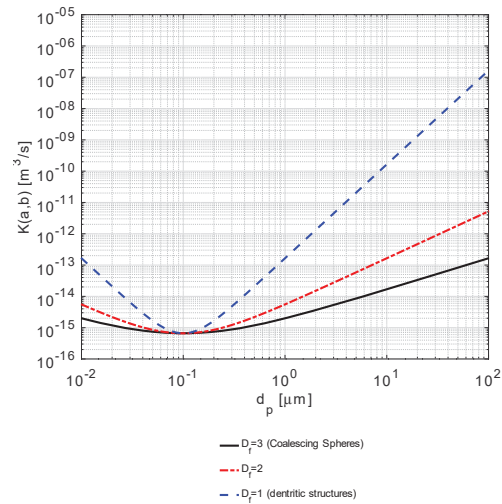


Fig. 7 Effects of non-spherical particles on coagulation (where  $D_f=3$  provides spherical particle, all other values indicate dentritic structures)

6) *Size Distribution*: Because removal processes are involved in the problem the size distribution statistical parameters will change with time (i.e. no self similar solution exists). Therefore the selection of an approximate form of the size distribution is key to the coagulation solution. For a single source term (assumed here) and a single species of aerosol, the lognormal distribution provides a reasonable approximation and results in a simple set of analytical equations to assist in evaluating the dynamic aerosol balance equation using the method of moments [4, 20].

### B. Removal Mechanisms

Aerosol removal from within the package ullage space occurs due to deposition, gravitational settling and leakage to the environment. The models used to implement these removal processes are discussed next.

1) *Gravitational Settling*: The gravitational settling removal term,  $R_g$ , is calculated as follows [4]:-

$$R_g = S_g C_g(v) = S_g \frac{\rho_p g}{18\mu} \left( \frac{6}{\pi} \right)^{2/3} \quad (16)$$

where:-

$$\begin{aligned} S_g &= \text{Ratio of gravitational settling surface area} \\ &\quad \text{to gas volume} \\ \rho_p &= \text{Particle density} \\ \mu &= \text{Dynamic viscosity of gas} \\ C_g(v) &= \text{Gravitational settling velocity of particles} \\ &\quad \text{in Stoke's flow} \end{aligned}$$

Equation 16 is valid for  $Re < 1$  and  $d_p > 1\mu\text{m}$  [16].

To deal with particles  $< 1\mu\text{m}$  a slip correction factor can be applied to 16 to adjust their gravitational settling velocity. This correction factor is not used in this model but is worthy of discussion as it shows that by omitting it, gravitational settling is treated in a conservative way.

To extend the range of applicability down to  $0.1 \mu\text{m}$  the Cunningham slip correction factor is calculated as [16]:-

$$C_c = 1 + \frac{2.52l_p}{d_p} \quad (17)$$

$C_c$  is always greater than 1 and is applied as a multiplier on  $C_g$ , 16. Therefore its effect is to increase gravitational settling velocity, thereby increasing loss of particulate due to gravity and reducing loss to the environment.

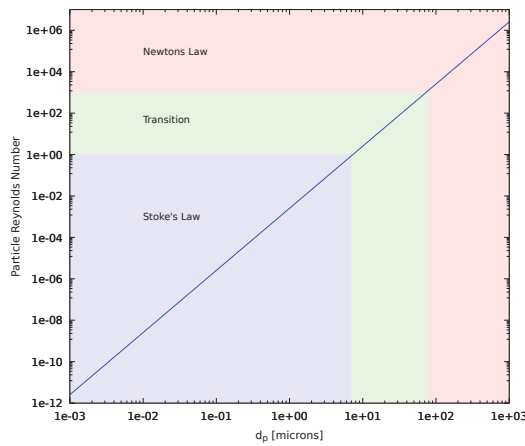


Fig. 8 Particle Reynolds number (based on Stokes law) plotted against particle diameter

To assess the effects of particles with a Reynolds number greater than 1 the particle Reynolds number based on Stokes law was calculated for particles ranging in size from 1nm to 1mm following a method proposed by Hinds [16]. The results of the calculations are shown in Fig. 8. The figure indicates that at particle sizes greater than 7 microns the particle Reynolds number exceeds 1. To correct the gravitational settling velocity in a transition flow a second graph was produced, see Fig. 9. This figure compares the gravitational settling velocity based on Stokes law (blue line) and a "corrected" gravitational settling velocity due to  $Re > 1$  (red line). Based on initial SLR calculations a maximum capillary diameter of  $\approx 60 \mu\text{m}$  is assumed to be present during ACT so it is evident that in the size range of interest ( $< 100 \mu\text{m}^2$ ) there is negligible difference between the velocity curves. For this reason 16 will be applied without further modification.

<sup>2</sup>It is assumed that the upper bound particle size limit of  $100 \mu\text{m}$  will be justifiable by SLR measurement

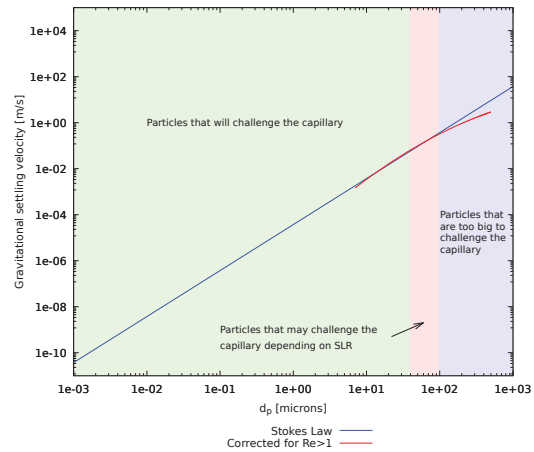


Fig. 9 Comparison of gravitational settling velocity equations

2) *Brownian Deposition:* Removal of particulate due to Brownian deposition is modelled with [21]:-

$$R_b(v) = \frac{S_b}{4.6} D_B(v)^{0.735} \quad (18)$$

where:-

$S_b$  = Ratio of Brownian deposition settling area to gas volume

$D_B(v)$  = Brownian diffusion coefficient

3) *Seal Leakage:* The effects of capillary plugging have not been considered in the model, eliminating uncertainty and increasing pessimism in the approach. Particles in this model can grow bigger than the maximum possible capillary diameter (for the specified SLR) and still be released to the environment - if they do not fall out of gas suspension first.

To calculate the removal constant for leakage,  $R_l$ , an estimated SLR,  $L_x$  is proposed for the package as  $5 \times 10^{-4} \text{ Pa.m}^3.\text{s}^{-1}$  in ACT and  $1 \times 10^{-4} \text{ Pa.m}^3.\text{s}^{-1}$  in NCT. A leak rate adjusted to transport conditions of temperature and pressure ( $\text{Pa.m}^3.\text{s}^{-1}$ ),  $L_y$ , can then be calculated and from this a volumetric leakage rate and the leakage term  $R_l$  determined.

Beginning with Equation B.2 from ISO12807 [2]:-

$$L_x = L_y \frac{\mu_y (p_u^2 - p_d^2)_x}{\mu_x (p_u^2 - p_d^2)_y} \quad (19)$$

and rearranging to solve for  $L_y$ :-

$$L_y = L_x \left( \frac{\mu_y (p_u^2 - p_d^2)_x}{\mu_x (p_u^2 - p_d^2)_y} \right)^{-1} \quad (20)$$

A volumetric leak rate is then calculated by dividing by package pressure:-

$$Q_f = \frac{L_y}{p_f} \quad (21)$$

and the leakage rate removal term  $R_l$  is finally calculated as:-

$$R_l = \frac{Q_f}{V_{gas}} \quad (22)$$

It is noteworthy that there is no dependence on particle size for leakage but there is for the other removal processes, gravitational settling and Brownian deposition. As a consequence both  $R_g$  and  $R_b$  vary with time as the particle size changes whilst  $R_l$  remains constant.

### C. Condensation and Evaporation

Two further aerosol processes that may occur are condensation and evaporation. If condensation occurs this enhances growth rate of particulate and therefore omitting it from this solution is conservative. For particle evaporation to occur temperatures far in excess of the expected maximum of 160°C are required so it is safely assumed that evaporation will not occur during NCT or ACT. Therefore the effects of condensation and evaporation are not modelled.

### D. Mechanical Resuspension

It is possible to model the resuspension of particulate that has settled or deposited on the internal surfaces which would result in slower attenuation of the source term as particulate is reintroduced into the flow. Resuspension occurs in turbulent flows and calculation requires a force balance between adhesive forces and aerodynamic forces acting on particles. For the preparation of this model it is assumed that any turbulence generated will not cause gross resuspension of the settled out particulate.

### E. Source Term

At time=0 a pulse (delta function) of releasable material (releasable fraction) is injected into the ullage space gas within the package. It is postulated that this arises from mechanical damage to the HAW during an impact accident and is a polydisperse, well stirred mixture. In the NCT case the source term is derived from the maximum permissible surface contamination of the waste package. The present work treats the entire source term as solid particulate.

## IV. SOLUTION METHOD

By definition  $\phi(t) = N(t)\bar{v}(t)$  so to solve the dynamic aerosol balance equation at least two equations are required to solve for both  $N(t)$  and  $\phi(t)$ . Because the size distribution statistical parameters are also unknown a third equation is required for  $\sigma$  the geometric standard deviation of the lognormal distribution. To evaluate the size distribution integral the method of moments is applied [4]. This results in a set of three, coupled ordinary differential equations:-

$$\frac{dN(t)}{dt} = K_B N^2 - R_m \phi^m N^{1-m} \exp(m(m-1)\sigma/2) \quad (23)$$

$$\frac{d\phi}{dt} = -R_m \frac{\phi^{m+1}}{N^m} \exp(m(m+1)\sigma/2) \quad (24)$$

$$\begin{aligned} \frac{d\sigma}{dt} = & K_B N (1 + \exp(\sigma/9)) (2\exp(-\sigma) - 1) \\ & + R_m \left( \frac{\phi^m}{N} \right) \left\{ 2\exp(m(m+1)\sigma/2) \right. \\ & \left. - \exp(m(m-1)\sigma/2) - \exp(m(m+3)\sigma/2) \right\} \end{aligned} \quad (25)$$

where:-

- 1)  $m = 2/3$  for gravitational settling
- 2)  $m = -1/3$  for Brownian deposition
- 3)  $m = 0$  for leakage

The volume fraction released from the package can then be related to the activity released to the environment. The solution of these equations is currently being implemented in a computer program called: Activity Release Calculator (ARC).

## V. COMPARISON OF THE APPROACH WITH THE ISO12807 METHODOLOGY

Fig. 10 provides a flow chart for the gas leakage methodology described in ISO12807 [2]. The first 9 steps are used for determining a permissible standardised leak rate by relating the activity of the contents to the potential egress of material from the package either by by-pass leakage or permeation of the seal. These steps included methods for dealing with activity of each phase; gas, liquid or solid. In the case of solids the method involves the calculation of a maximum permissible capillary diameter; which is used when the particle size distribution is known to enable a case for capillary plugging.

Step 10 converts the permissible standardised leakage rate to a test leakage rate for each verification stage; design, fabrication, preshipment, periodic and maintenance. A test method is then selected and a test performed in step 11 to demonstrate containment.

The proposed method in this paper is based on ISO12807 but differs in a few significant ways. Fig. 11 provides a flow chart to show how the method could be incorporated into ISO12807. Step 1 commences by listing the radionuclides within the waste package(s). Step 2 identifies a releasable fraction of solids. Step 3 then specifies an SLR (which ISO12807 permits) and from this steps 3 - 6 calculate the activity release rate for solids that can be released from the package due to by-pass leakage. The approach to safety of active gas releases is confirmed by comparison against screening limits, but if required, it is possible to expand this method to account for active gases and liquids using the current ISO12807 methodology. The focus of this paper is limited to the release of solid particulate.

## VI. MODEL VALIDATION

The simplest approach to validation is a direct comparison of an experiment of the scenario with the ARC model. This is excluded as an option for the following reasons:-

- 1) The replication of the accident scenario and measurement of activity (or mass) release is not feasible



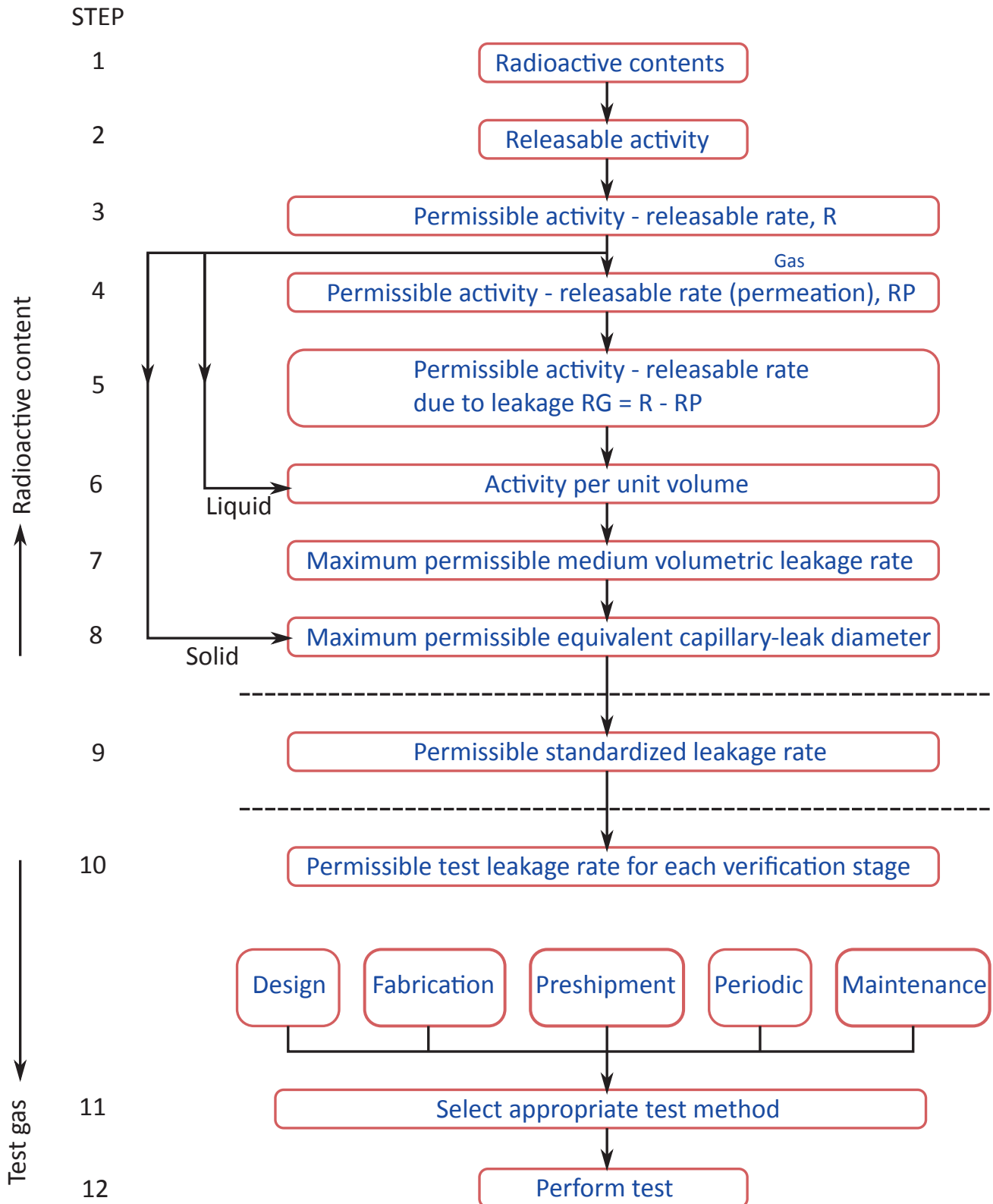


Fig. 10 ISO12807 Gas leakage methodology [2]

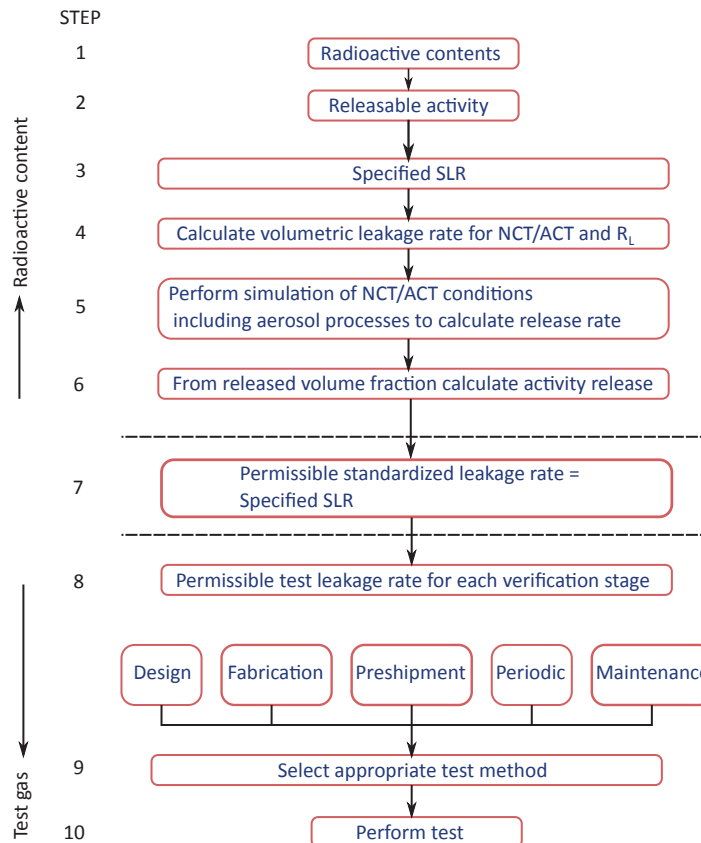


Fig. 11 Modified ISO12807 methodology to account for aerosol behaviour

- 2) The proposed model is simplistic and any experiment would introduce additional complexity requiring model modification. Therefore results will not agree. However, they would serve to demonstrate that the approach is conservative

Therefore an indirect approach to model validation is considered based on expert peer review, indirect “building blocks” type experiments and alternative calculation methods. In particular work is beginning on developing a seal test rig to underpin the specified SLR and waste inventory characterisation will assist in understanding the extent of the problem and the reliance on ARC. Also a programme of work through the UK University system will be undertaken to develop options for providing evidence by analogy, test and experiment to support the additional modelling of aerosol processes in the containment assessment.

## VII. CONCLUSION

In this paper an approach to nuclear transport package containment safety cases has been proposed that includes the consideration of aerosol processes. The dynamic aerosol balance equation has been evaluated with respect to the anticipated conditions within a transport package. Wherever possible, lower bound values have been applied and potentially beneficial physical processes excluded because there is either

a degree of uncertainty over whether they will be present in the containment or simply to remain conservative.

## VIII. FUTURE WORK

Future work includes the completion of the ARC model, further waste inventory characterisation and a university based literature review specifically focusing on the additional arguments based on modelling of aerosol processes to assist with model validation. Additionally separate work could be conducted to confirm the current assumption that the releasable fraction from the impact accident dominates that produced due to a thermal accident.

## ACKNOWLEDGMENT

The authors would like to thank Professor Mike Reeks and Professor Mike Williams for their assistance with the theoretical background to this work.

## ACRONYMS

ACT	Accident Conditions of Transport
ARC	Activity Release Calculator
GDF	Geological Disposal Facility
HAW	Higher Activity Waste
IAEA	International Atomic Energy Agency
ILW	Intermediate Level Waste
INS	International Nuclear Services
NCT	Normal Conditions of Transport
NDA	Nuclear Decommissioning Authority

RAM Radioactive Material  
 RWM Radioactive Waste Management  
 SLR Standardised Leak Rate  
 SWTC Standard Waste Transport Container

## NOMENCLATURE

$A_2$  = Quantity (activity) of radioactive material [Bq]  
 $Bq$  = Becquerels (or decays per second)  
 $C_g$  = Gravitational settling velocity [ $\text{m.s}^{-1}$ ]  
 $D_B$  = Brownian diffusion coefficient [ $\text{m}^2.\text{s}^{-1}$ ]  
 $\epsilon_T$  = Turbulent intensity [ $\text{m}^2.\text{s}^{-3}$ ]  
 $I(v, t)$  = Rate of growth/loss of particles due to condensation or evaporation  
 $k$  = Boltzmann's constant  $1.38 \times 10^{-23}$  [ $\text{J.K}^{-1}$ ]  
 $K$  = Coagulation kernel [ $\text{m}^3.\text{s}^{-1}$ ]  
 $K_B$  = Brownian coagulation kernel [ $\text{m}^3.\text{s}^{-1}$ ]  
 $l$  = Length of turbulent eddies [m]  
 $l_p$  = Mean free path [m]  
 $L_x$  = Standardised leak rate [ $\text{Pa.m}^3.\text{s}^{-1}$ ]  
 $L_y$  = Leak rate in transport conditions (measured) [ $\text{Pa.m}^3.\text{s}^{-1}$ ]  
 $n(v, t)$  = Number of particles as a function of volume and time  
 $N(t)$  = Particle number density [ $\text{m}^{-3}$ ]  
 $p_d$  = Downstream pressure [Pa]  
 $p_f$  = Package internal pressure [Pa]  
 $p_u$  = Upstream pressure [Pa]  
 $Q_f$  = Volumetric leak rate [ $\text{m}^3.\text{s}^{-1}$ ]  
 $R$  = Removal terms  
 $R_b$  = Brownian deposition removal term [ $\text{s}^{-1}$ ]  
 $R_g$  = Gravitational removal term [ $\text{s}^{-1}$ ]  
 $R_l$  = Leakage removal term [ $\text{s}^{-1}$ ]  
 $S_g$  = Surface area / gas volume for gravitational settling  $\text{m}^{-1}$   
 $S_b$  = Surface area / gas volume for Brownian deposition  
 $S(v, t)$  = Source term  
  
 $T$  = Temperature [K]  
 $\bar{u}$  = Root mean square velocity [ $\text{m.s}^{-1}$ ]  
 $v$  = Particle volume [ $\text{m}^3$ ]  
 $V_{gas}$  = Volume of gas [ $\text{m}^3$ ]  
 $\bar{v}$  = Average particle radius [m]  
 $\nu$  = Kinematic viscosity [ $\text{m}^2.\text{s}^{-1}$ ]  
 $\mu$  = Dynamic viscosity [ $\text{N.s.m}^{-2}$ ]  
 $\mu_x$  = Gas viscosity in transport conditions [ $\text{N.s.m}^{-2}$ ]  
 $\mu_y$  = Gas viscosity in standard conditions [ $\text{N.s.m}^{-2}$ ]  
 $\rho_p$  = Particle density [ $\text{kg.m}^{-3}$ ]  
 $\rho_m$  = Molecular density [ $\text{kg.m}^{-3}$ ]  
 $\sigma$  = Standard deviation of lognormal distribution  
 $\sigma_{air}$  = Diameter of air molecules [m]  
 $\phi(t)$  = Volume fraction

## REFERENCES

- [1] IAEA Safety standards for protecting people and the environment, Regulations for the safe transport of radioactive material. 2018 Edition.
- [2] BS ISO 12807:2018. BSI Standards Publication, Safe transport of radioactive materials - Leakage testing on packages. 2018.
- [3] S. Friedlander. *Smoke, dust, and haze, fundamentals of aerosol dynamics*. Oxford University Press, Second Edition, 2000.
- [4] M.R.R. Williams and S.K. Loyalka. *Aerosol science theory and practice with special applications to the nuclear industry*. Pergamon Press, First Edition, 1991.
- [5] M.R.R. Williams. Some topics in nuclear aerosol dynamics. *Progress in Nuclear Energy*, 17:1–52, 1986.
- [6] F. Cousin, M.P. Kissane, and N. Girault. Modelling of fission-product transport in the reactor coolant system. *Annals of Nuclear Energy*, 61:135–142, 2013.
- [7] T. Haste, F. Payot, and P.D.W. Bottomley. Transport and deposition in the Phébus FP circuit. *Annals of Nuclear Energy*, 61:102–121, 2013.
- [8] M. Schwarz, G. Hache, and P. von der Hardt. PHEBUS FP: a severe accident research programme for current and advanced light water reactors. *Nuclear Engineering and Design*, 187:44–69, 1999.
- [9] H.J. Allelein, A. Auvinen, J. Ball, S. Guntay, L. Herranz, A. Hidaka, A.V. Jones, M.P. Kissane, D. Powers, and G. Weber. State-of-the-art report on nuclear aerosols in reactor safety. Technical Report NEA/CSNI/R(2009)5, Nuclear Energy Agency - Committee on the Safety of Nuclear Installations, 2009.
- [10] S. Chatzidakis. Stress corrosion cracking aerosol transport model summary report. Technical Report ORNL/SPR-2018/1072, Oak Ridge National Laboratory (ORNL), 2018.
- [11] C.F. Clement. Aerosol penetration through capillaries and leaks: theory. *Journal of Aerosol Science*, 26(3):369–385, 1995.
- [12] D.A. Morton and J.P. Mitchell. Aerosol penetration through capillaries and leaks: Experimental studies on the influence of pressure. *Journal of Aerosol Science*, 26(3):353–367, 1995.
- [13] M. Tian, H. Gao, X. Han, Y. Wang, and R. Zou. Experimental study on the penetration efficiency of fine aerosols in thin capillaries. *Journal of Aerosol Science*, 111:26–35, 2017.
- [14] R. Martens, F. Lange, W. Koch, and O. Nolte. Experiments to quantify airborne release from packages with dispersible radioactive materials under accident conditions. *EuroSafe Conference*, 2005.
- [15] W. Koch, F. Lange, R. Martens, and O. Nolte. Determination of accident related release data. *14th International Symposium on the Packaging and Transportation of Radioactive Materials PATRAM*, 2004.
- [16] W.C. Hinds. *Aerosol technology: Properties, behavior, and measurement of airborne particles*. John Wiley and Sons, Second Edition, 1999.
- [17] S.H. Park, F.E. Kruis, K.W. Lee, and Fissan H. Evolution of Particle Size Distributions due to Turbulent and Brownian Coagulation. *Aerosol Science and Technology*, 36:419–432, 2002.
- [18] A.M. Shahub and M.R.R. Williams. The importance of collision efficiency in the coagulation of nuclear aerosol particles. *Nuclear Technology*, 86:80–86, 1989.
- [19] A.M. Shahub and M.R.R. Williams. Brownian collision efficiency. *Journal of Physics D: Applied Physics*, 21:231–236, 1998.
- [20] M.R.R. Williams. On the modified gamma distribution for representing the size spectra of coagulating aerosol particles. *Journal of Colloidal Interface Science*, 103:516–527, 1985.
- [21] J.F. van de Vate. Investigations into the dynamics of aerosols in enclosures as used for air pollution studies. Technical report, Netherlands Energy Research Foundation Report ECN-86, 1980.